Pillared clays from natural resources as catalysts for catalytic wet peroxide oxidation: Characterization and kinetic insights

Marzhan Seitovna Kalmakhanova[1], Jose Luis Diaz de Tuesta[2,3†],

Bakytgul Kabykenovna Massalimova[1], Helder Teixeira Gomes[2,3†]

[1]Department of Chemistry and Chemical Engineering, M.Kh. Dulati Taraz State University, Taraz, Kazakhstan
[2]Mountain Research Center CIMO, Polytechnic Institute of Bragança, 5300-253 Bragança, Portugal
[3]Laboratory of Separation and Reaction Engineering – Laboratory of Catalysis and Materials (LSRE-LCM), Faculty of Engineering of the University of Porto (FEUP), Rua Dr. Roberto Frias, 4200-465 Porto, Portugal

ABSTRACT

Pillared clays with Zr and Fe/Cu/Zr polycations have been prepared from natural clays found in large deposits of Kazakhstan and assessed as catalysts for the catalytic wet peroxide oxidation (CWPO), using 4-nitrophenol (4-NP) as model compound. The performance of the catalysts was followed by measuring the concentration of 4-NP, H_2O_2 and the total organic carbon (TOC), considering C_{4-NP} = 5 g L^{-1}, $C_{H_2O_2}$ = 17.8 g L^{-1}, C_{cat} = 2.5 g L^{-1}, initial pH = 3.0 and T = 50°C. At those selected conditions, the pillared clays showed higher activity than natural clays in the CWPO of 4-NP. The conversion of the model pollutant was complete when Fe/Cu/Zr-PILCs were used, with the TOC removal reaching 78.4% after 24 h with the best Fe/Cu/Zr-PILC. The H_2O_2, 4-NP and TOC time-evolution was well described by a kinetic model based on TOC lumps in three blocks, considering the initial TOC (corresponding to 4-NP), the production of oxidizable intermediates and the formation of refractory products.

Keywords: Advanced oxidation process, Clay-based catalyst, CWPO, Kinetic modeling, Wastewater treatment, 4-nitrophenol

1. Introduction

In modern life, especially in productive activities, water plays an important role. There are about 39 thousand rivers and temporary streams in Kazakhstan. Among them, over 7 thousand are more than 10 km long. Most of the rivers in Kazakhstan belong to the internal closed drainage basins of the Caspian and Aral Seas and Balkhash, Alakol and Tengiz Lakes [1]. The majority of industries are situated around these rivers and lakes in order to use the water and to enable the discharge of some effluents for the aquatics systems. However, some of those streams can be harmful, making nowadays the contamination one of the primary issues of environmental authorities, requiring solutions in order to reduce its impact by using effective and inexpensive wastewater treatment methods, such as advanced oxidation processes (AOPs).

Nowadays, the scientific community shows an increasing interest in the development of AOPs (e.g., Fenton process, photo catalytic oxidation and electro catalytic oxidation) for the removal of recalcitrant and non-biodegradable organic compounds from aqueous streams. AOP are particularly useful technologies to treat recalcitrant or non-degradable compounds present in wastewaters in a wide range of concentrations (0.1-10 g/L) [2,3], difficult to remove by the conventional biological processes. The Fenton process consists on the use of iron and hydrogen peroxide, commonly known as Fenton's reagent (H_2O_2 + Fe^{2+}), for the generation of hydroxyl radicals (E_0^o = 2.80 V), highly oxidizing species capable of degrading the organic matter present in wastewater effluents. The loss of the homogeneous catalyst is a major drawback that limits in practice the application of the Fenton process [4], since there is the necessity of a continuous feeding of iron and the corresponding additional separation processes and sludge disposal. In addition, although the Fenton process can completely destroy organic pollutants to harmless products, it requires a tight range of pH to operate (typically between 2 and 3, depending on the effluent [5]), and the need

for further recovery of the precipitated catalyst [5,6], reducing its popularity to be applied widely in industries. In order to avoid the inconveniences found in Fenton oxidation, in the last decades researchers have tested a variety of heterogeneous catalysts as alternatives, using hydrogen peroxide as an oxidizing agent. The oxidation process with H_2O_2 considering a heterogeneous catalyst in commonly known as catalytic wet peroxide oxidation (CWPO). CWPO is one of the promising methods for the removal of organic pollutants at mild temperature and pressure conditions [7,8], providing that a suitable catalytic system is used, such as catalysts based on natural and pillared clays (PILCs).

PILCs are porous materials developed by molecular design methods, obtained by exchanging the cations of alkaline and alkaline earth metals, located in the interlayer space of clays, by inorganic polyoxo (hydroxo) cations. To prepare PILCs, intercalating salt solutions of Al, Cu, Cr, Zr, Fe, Zn and other active metals are usually used [8-10]. The use of these metals, combined as polyoxycations, are of greatest interest since they lead to high thermal stability [9]. By changing the nature and, hence, the size of the pillars, different pore-sizes are obtained; and it becomes possible to tune the porosity. This porosity, coupled with the properties of different pillars and host, are very important for certain applications [9]. Previous work shows that the intercalation of different pairs of cations on natural clays, as zirconium (Zr), copper (Cu), iron (Fe), leads to improved catalytic activity for the oxidation of organic compounds, mainly tested with phenol, extensively used as model pollutant [10]. In CWPO, PILCs have been used as catalysts, taking advantage of its porous structure to adsorb organic compounds on its surface, which actively participates in the oxidation process in the presence of hydrogen peroxide. The use of 4-nitrophenol (4-NP) as model compound to assess the performance of catalytic systems in AOPs has been less explored than phenol, the mechanistic insights lacking consolidated data. However, few reports in CWPO [11-14], photo oxidation by UV/H_2O_2 [15] and, in previous works on our group by CWPO with reduced graphene oxide materials [16], magnetic carbon xerogels [17] and carbon nanotubes [2], reveal that the main reaction intermediates are hydroquinone, benzoquinone, catechol and several low molecular weight carboxylic acids (e.g., malonic, malic, maleic and acetic acids). To the best of our knowledge, there are no works related to the development of kinetic models for the CWPO of 4-NP and nowadays most of the studies regarding CWPO processes present only pseudo-first order rate equations describing the disappearance of a target pollutant [18].

4-NP is a toxic and bio-refractory compound that can damage the central nervous system, liver, kidney and blood of humans and other living beings. It has been shown in the literature that 4-NP can develop a blood disorder which reduces the ability of the blood to carry oxygen to tissues and organs [19,20]. Thus, the use of 4-NP as model compound in AOP studies and the knowledge of its degradation mechanism and kinetics are of highly importance.

In this study, we report the results obtained in the CWPO of 4-NP in aqueous reaction media (used as model synthetic wastewater) considering monometallic (Zr) and trimetallic (Fe/Cu/Zr) PILCs prepared from natural clays extracted from Akzhar and Karatau (Kazakhstan) deposits, using zirconium tetrachloride, copper sulphate and ferrous sulphate as pillaring cation precursors. The catalytic activity of the prepared PILCs is compared to the extracted natural clays and a kinetic model is developed for the CWPO of 4-NP.

2. Materials and Methods

2.1. Reagents and Chemicals

Clays were obtained from the Karatau and Akzhar deposits (located in the Zhambyl region of south of Kazakhstan). Zirconium tetrachloride, reactor grade (99.5 %), was supplied from Alfa Aesar, and ferrous sulphate heptahydrate (99.5%) and copper sulphate pentahydrate (99.9%) were obtained from Skat reactives. Hydrogen peroxide (30% w/v), used as oxidant in the treatment of the synthetic wastewater, was purchased from Fluka. Titanium (IV) oxysulphate (TiOSO$_4$, 15 wt.% in dilute sulphuric acid, 99.99%), hydrochloric acid (HCl, 37 wt.%) and sodium sulphite (Na$_2$SO$_3$, 98 wt.%) were purchased from Sigma-Aldrich. Sodium hydroxide (NaOH, 98 wt.%) was obtained from Panreac. 4-NP (98 wt.%) and 4-nitrocatechol (98 wt.%) were acquired from Acros Organics and Fluka, respectively. Methanol (HPLC grade), glacial acetic acid (analytical reagent grade) and acetonitrile (HPLC grade) were obtained from Fisher Chemical. All chemicals were used as received without further purification. Distilled water was used throughout the work.

2.2. Preparation of Pillared Clays

Two natural clays extracted from Karatau (KNC) and Akzhar (ANC) deposits were used as raw materials to prepare the pillared clays. First, the extracted natural clays were extensively washed with HCl (2 M) at 50ºC, in order to eliminate non-bonded content of metal and other contaminants present inside the clays. Pillared clays were then prepared from the washed natural clays, using zirconium tetrachloride as a source of zirconium polycations. Ferrous sulphate and copper sulphate were used as source of iron and copper polycations. The pillaring solution was prepared by slow addition of NaOH (0.2 M) to the solution containing the polycation precursors at room temperature until pH = 2.8 were obtained. The resultant solution was aged for 24 h at room temperature. The clay pillaring process kept a ratio of 10 mmol of total metal per gram of washed clay, irrespective Zr-PILCs or Fe/Cu/Zr-PILCs were prepared. The final materials were dried at 350 K for 24 h and calcined during 2 h at 823 K considering a heating rate of 275 K min^{-1}.

2.3. Characterization Methods

The physico-chemical characteristics of the natural and pillared clays were determined by X-ray spectral analysis performed with a spectrometer Inca Energy from Oxford instruments, using an electron microprobe (EMP) of the brand Superprobe 733 from JEOL. X-ray diffraction analysis was performed on an automated diffractometer DRON-3 with CuKa - radiation, β-filter. A semiquantitative basis was carried out on the diffraction patterns of powder samples using the method of equal weights and artificial mixtures. The diffraction patterns were interpreted using ICDD data: a base of powder diffractometric data PDF2 (Powder Diffraction File) and diffractograms of mineral-free impurities with the EVA program version 7.0. Scanning electron microscope (SEM) was performed on a FEIQuanta 400FEG ESEM/EDAX Genesis X4M instrument equipped with an

energy dispersive spectrometer (EDS). Transmission electron microscopy (TEM) was performed in a LEO 906E instrument operating at 120 kV, equipped with a 4Mpixel 28 × 28 mm CCD camera from TRS.

The pH of point of zero charge (pH_{PZC}) was determined by pH drift tests, following the procedure described elsewhere [21,22]. Briefly, five NaCl (0.01 M) solutions were prepared as electrolyte and initial pH was adjusted to 2, 4, 6, 8 and 10 using HCl and NaOH 0.1 M solutions. Then, samples of 0.05 g of pillared clays were loaded in each 20 mL of the previous solutions. The equilibrium pH of each suspension was considered after 48 h under stirring (320 rpm) at room temperature and, hence, the pH was measured (final pH). The pH_{PZC} value was determined by intercepting the curve 'final pH vs initial pH' with the straight line 'initial pH = initial pH'. Fourier Transform Infrared Spectroscopy (FTIR) spectra of natural and PILCs were obtained with a FTIR instrument (Infraspek, Model FSM 1201, Russia, St-Petersburg) with a resolution of 1 cm^{-1} and scan range of 7,800 to 400 cm^{-1} using a sample based on 1% of clay with KBr.

2.4. Catalytic Runs

The CWPO of 4-NP in aqueous medium was carried out in a 250 mL well-stirred glass reactor maintained at 323 K. The reactor was loaded with 100 mL of a concentrated (5.0 g/L) 4-NP aqueous solution, considered as a model system to simulate high-loaded wastewaters [2,23-25]. The initial pH of the solution was adjusted to 3 by adding H_2SO_4 and NaOH solutions (not buffered). The stoichiometric quantity of hydrogen peroxide needed for complete mineralization of 4-NP was then added. The catalyst was loaded (2.5 g/L) after homogenization of the resulting solution, that moment being considered as $t_0 = 0$ h. All experiments were carried out during 24 h. Several samples were withdrawn from the medium of reaction at previously selected reaction times to follow the course of the 4-NP conversion and the appearance of intermediate compounds, measured by high-performance liquid chromatography (HPLC). For that purpose, a Jasco HPLC system equipped with a UV-Vis detector (UV-2075 Plus), a quaternary gradient pump (PU-2089 Plus) for solvent delivery (1 mL min^{-1}) and a Kromasil 100-5-C18 column (15 cm × 4.6 mm; 5 μm particle size; reversed-phase) was employed. Total Organic Carbon (TOC) and H_2O_2 concentrations were also measured during each run, using respectively a Shimadzu TOC-L CSN analyzer and a colourimetric method based on $TiOSO_4$ [16].

2.5. Kinetic Modelling

The kinetic modelling of the CWPO results obtained with the natural clays Karatau and Akzhar and with the PILCs Fe-Cu-Zr-Karatau and Fe-Cu-Zr-Akzhar has been performed to describe the time-course evolution of 4-NP (used as target pollutant), H_2O_2 and TOC concentrations, following the procedures described elsewhere [18,22]. The rate of disappearance of each given compound (i) in the reaction medium, r_i (mol g^{-1} s^{-1}), is given by Eq. (1):

$$-r_i = \frac{1}{C_{cat}} \frac{dC_i}{dt} \tag{1}$$

where C_{cat} refers to the catalyst concentration (g L^{-1}), C_i to the concentration of compound i, such as H_2O_2, 4-NP or TOC (mol

L^{-1}) and t representing the time of reaction (h). The rate of disappearance r_i can be expressed as a function of the concentration of the species involved in the reaction.

The numerical integration of the rate equations was solved by using the Microsoft Excel Solver (Microsoft Office 2010, Microsoft Corp.) for least-squares minimization. The models were also evaluated by the sum of square residual (SSR) and determination factor (R^2), calculated by applying Eq. (2) and Eq. (3), respectively:

$$SSR = \Sigma_{n=1}^{N} \left(C_{exp\ i,n} - C_{model\ i,n} \right)^2 \tag{2}$$

$$R^2 = \frac{\Sigma_{n=1}^{N} \left(C_{model\ i,n} - \overline{C_{model\ i}} \right)^2}{\Sigma_{n=1}^{N} \left(C_{model\ i,n} - \overline{C_{model\ i}} \right)^2 + \Sigma_{n=1}^{N} \left(C_{exp\ i,n} - \overline{C_{model\ i,n}} \right)^2} \tag{3}$$

3. Results and Discussion

3.1. Characterization of the Natural Clays and PILCs

3.1.1. X-Ray diffraction

The powder X-ray diffraction patterns of the natural clays are shown in Fig. 1. In the diffractogram of the natural clays, the peaks at 2θ = 6.2° (d$_{001}$-14.19 Å) and 2θ = 19.9° (d = 4.5 Å) represents the characteristic reflection of montmorillonite (represented as M in Fig. 1), as reported by Is Fatimah [26]. The diffraction peaks at (2θ) 20.85°, 26.6°, 36.5°, 39.5° and 50.1° revealed the presence of quartz (as Q in Fig. 1), an impurity in the natural clays [13,26]. The reflections at (2θ) 23.01°, 29.5° and 36.0° was due to calcite (represented as C in Fig. 1) [27].
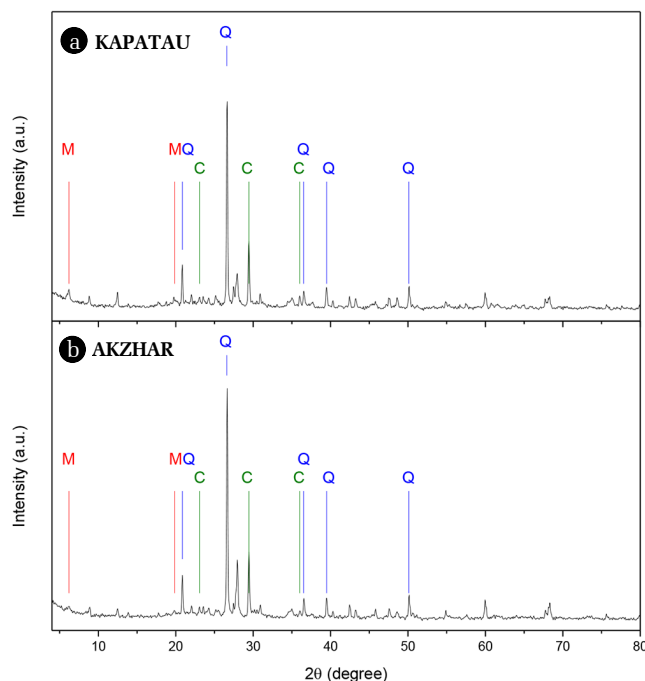

Fig. 1. X-ray diffraction spectra obtained for (a) KNC and (b) ANC (M: montmorillonite, Q: quartz, C: calcite).

Table 1. Chemical Composition of the Natural and Pillared Clays, Determined by Elemental Analysis

Clay	Mass of the element (%)										
	Na	Mg	Al	Si	K	Ca	Ti	Mn	Fe	Cu	Zr
KNC	1.7	4.8	13.9	44.8	4.8	16.2	3.4	0.5	9.9	n.i.*	n.i.*
ANC	1.8	4.9	13.2	48.4	4.8	18.3	0.7	n.i.*	7.9	n.i.*	n.i.*
Zr-APILC	2.0	2.5	9.8	40.5	4.8	0.8	0.5	n.i.*	2.8	n.i.*	36.3
Zr-KPILC	2.5	2.5	10.0	41.8	4.3	0.9	0.3	n.i.*	2.7	n.i.*	35.0
Fe/Cu/Zr-KPILC	3.7	3.3	13.4	47.5	3.9	1.3	0.7	n.i.*	11.5	9.6	5.1
Fe/Cu/Zr-APILC	1.9	2.6	11.9	46.4	5.6	1.2	0.6	n.i.*	22.8	6.1	0.9

*n.i. = not identified

A semi-quantitative analysis was carried out from the XRD spectra in order to determine the composition of the natural clays in quartz, muscovite, feldspar, calcite, hydrated aluminum silicate and Kaolinite was determined (Table S1). As can be observed, these natural clays contain a high quantity of impurities in form of quartz and calcite (56.7 and 45.9% for ANC and KNC, respectively).

The content of quartz on raw natural clays can be different depending on the deposit of the clay. Djeffal et al. [28] reported the use of natural clay with 53.86% in quartz in the CWPO of phenol. The calcite presented in the raw clays is normally replaced during cation exchange in the pillaring process, as done in this work.

3.1.2. EMP

The chemical composition of the natural and pillared clays is shown in Table 1, as determined by Inca Energy with a dispersive spectrometer from Oxford Instruments. As observed, the natural clays used in this work are rich in iron (7.9-9.9%), which can play an important role in the decomposition of hydrogen peroxide to produce hydroxyl radicals for the oxidation of pollutants in CWPO. The analysis on the composition of the pillared clays indicates the successful enrichment of pillaring Zr cations in Zr-KPILC and Zr-APILC, by exchange with Ca cations. In Akzhar pillared clays the quantity of Zr is 36.3% and in Karatau pillared clay it is 35.1%. As expected, the content of Fe on the Fe/Cu/Zr-PILCs increases in the modified clays in comparison with the natural clays, suggesting the exchange and fixation of the intercalating metals in the interlayer space. This incorporation is particularly noticed on Fe/Cu/Zr-APILC, with the presence of 22.8% of Fe in the Fe/Cu/Zr-APILC, against 7.9% in the corresponding natural clay (ANC), whereas 11.5% of Fe was reached in the Fe/Cu/Zr-KPILC, against 9.9%. However, in the Fe/Cu/Zr-KPILC, the increment of Cu and Zr content was higher, reaching 9.6 and 5.1%, respectively; whereas 6.1 and 0.9% were achieved in the Fe/Cu/Zr-APILC. The total weight percentage in the three metals for Fe/Cu/Zr-APILC and Fe/Cu/Zr-KPILC resulted in 26.2 and 29.8%, respectively. It is also evidenced that the solids modified with Fe/Cu/Zr have lower Si/Al ratios (Si/Al < 3.7) than in the Zr-PILCs (Si/Al > 4.1), meaning that oxides got preferentially stabilized in the interlayer space of the clay, following the targeted cationic exchange mechanism [29]. Several works [13,14,30-32] dealing with different natural clays, modified with Al, Fe and Cu metal cations to produce pillared interlayered catalysts (Al/Fe, Al/Cu and Al/Cu/Fe), show to incre-

ment appreciably the catalytic activity of the respective natural clays in CWPO processes.

3.1.3. Fourier transforms infrared spectroscopy

The FTIR spectra of the ANC and of the APILCs are shown in Fig. 2. The general shape of all spectra is similar, indicating that the layered crystal structure of the natural clay is not strongly affected by the pillaring process. Peaks between the FTIR spectra of the pillared samples and of the natural clay suggest its successful modification.

The broad band at 3,444 cm^{-1} is due to bending and stretching vibrations of H_2O and the band at 1,631 cm^{-1} is due to an overtone of the bending vibration of water [33]. The band at 1,046 cm^{-1} is attributed to the stretching vibration of the Si-O bond, while the band corresponding to the bending vibration was observed at 875 cm^{-1}. The bending vibration bands of the Si-O-Si and Si-O bonds indicate that the natural clay holds two types of layered structures, one related to plane layer structure, and the other related to the interlayer structure with the appearance of the Si-O band at 536 cm^{-1}.

The absorption bands at 3,622, 2,922 and 2,852 cm^{-1} can be ascribed to –OH groups, typically found in other clays [33,34]. The presence of calcite in the raw material can be observed by the band found at 1,431 cm^{-1} [27]. This corroborates the presence of calcite in the natural clays observed by XRD analysis. As can be observed, the carbonate band significantly decreases after the pillaring process, likely due to exchange of the ions.
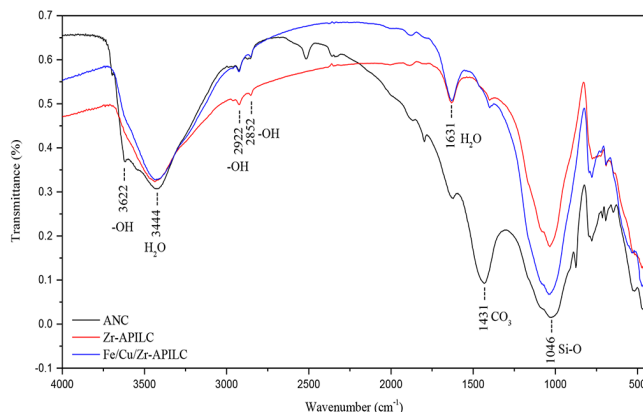
Fig. 2. FTIR spectra of ANC and APILCs.

3.1.4. Microscopy

The surface morphologies of the natural clays and of the PILCs prepared were observed by SEM and by TEM. In this work, SEM proves to be ideally suited for studying the configuration, texture of clay samples [35]. The corresponding SEM micrographs are shown in Fig. S1. Generally, the images of natural clays show layered and smooth surfaces. However, ANC and KNC (Fig. S1(A)-(B)) are not so smoother when compared to other non-pillared clays, such as the bentonite [33,36-40], whose surface is modified after pillarization showing a rougher surface and more porosity. The samples prepared by pillarization of ANC and KNC show a slight modification regarding the surface (slightly darker and rougher) and it is possible to observe higher particles when compared to the natural precursors.

The micrographs obtained by TEM analysis, in dark field mode, with natural and pillared clays are shown in Fig. 3. On the TEM images it is possible to observe characteristics of the materials, such as the stress, its crystallization, morphology and even its holography. On the TEM images of pillared clays shown in dark field mode the defects are evidenced, as well as fine particles present in the material, visible as dark-colored particles. These particles correspond to external aggregates of Zr which were used to modify the natural clays. This observation means that the impregnation of Zr on the natural clays also takes place along with its pillarization, likely due to an excess of the Zr precursor used. The phenomena has been also observed by other authors [41]. According with Fig.
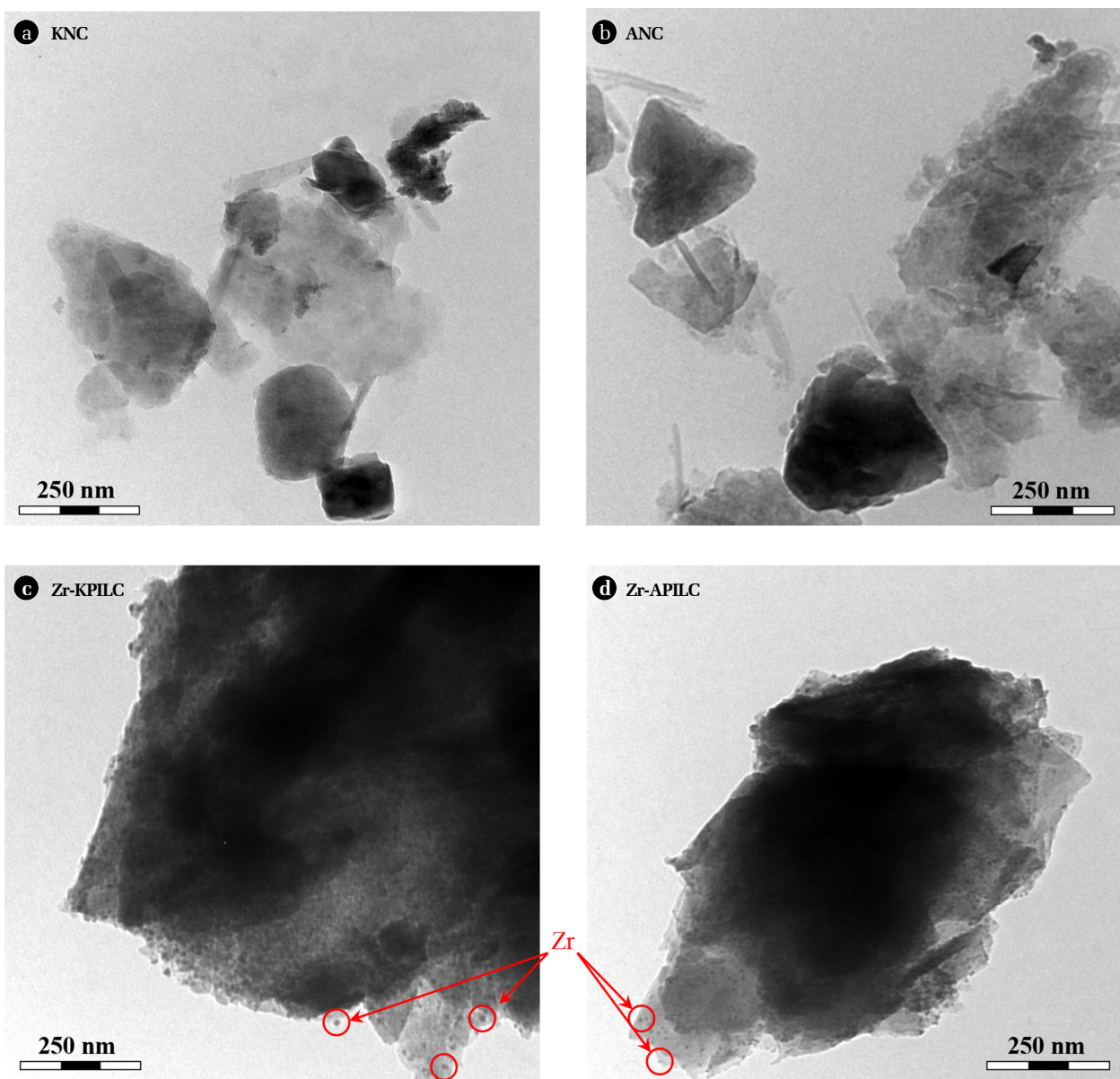

Fig. 3. TEM micrographs, in dark field mode, for (a-b) natural clays, (c-d) Zr-PILCs.

3, the Zirconia particles were highly dispersed on the natural clays, with some being anchored inside the natural materials. The Zr impregnation of the clays with high dispersion confers more active sites for the CWPO of 4-NP on the developed materials.

3.1.5. pH$_{PZC}$ determination

The pH at which the net total particle charge is zero is called the point of zero charge (pH_{PZC}), or pH_{PZC}, which is one of the most important parameters used to describe variable charge surfaces. The pH_{PZC} of the different natural clays and PILCs used in this work are shown in Table S2. The results reveal that ANC and KNC have clearly basic character, since the values of pH_{PZC} obtained for those clays were 9.3 and 9.1, respectively. However, the intercalation procedures used leads to a decrease of the basic character of the clays, resulting in pH_{PZC} values lower than 6.3 for all PILC materials. Concretely, the intercalation of Zr species produced a shift of pH_{PZC} from 9.3 (ANC) to 6.3 (Zr-APILC), and from 9.1 (KNC) to 6.1 (Zr-KPILC), for Akzhar and Karatau clays, respectively. Regarding the trimetallic Fe/Cu/Zr-PILCs, similar pH_{PZC} decreases were observed, shifts to 6.2 and 6.0 being obtained for Fe/Cu/Zr-Akzhar and Fe/Cu/Zr-Karatau pillared clays, respectively. These values are in good agreement with the pH_{PZC} values of Zr based pillared clays reported elsewhere [42]. The surface chemistry of the prepared PILC materials may thus be characterized as having a nearly neutral character which, when in contact with acidic aqueous solutions, will make the surface become with a positive charge, thus favorable for the attraction of negative anions present in solution.

3.2. CWPO of 4-NP

3.2.1. Screening of catalysts

Our work aims to develop affordable and active catalysts based on natural and pillared clays modified with Zr and Fe/Cu/Zr for use in purification processes of wastewaters containing organic pollutants by CWPO. Fig. 4(a) shows the conversion of 4-NP as a function of reaction time, obtained with the two natural clays and the four pillared clays considered in this work. The pillared clays were found to have excellent catalytic properties in the oxidation of 4-NP. It should be noted that the initial natural clay is rather inactive when compared to the modified materials (pillared clays). While the natural clays achieved only 32% of 4-NP conversion after 8 h of reaction, the materials modified with metals revealed 100% of 4-NP conversion in just 4 h of reaction. The materials modified with Fe/Cu/Zr species show better results than the solids modified with Zr species. While the conversions observed with the clays modified only with Zr reaches 100% after 4 h of reaction, the Fe/Cu/Zr-KPILC and Fe/Cu/Zr-APILC show 100% conversion of 4-NP in only 2 h of reaction. In all the experiments carried out with the natural clays, almost complete oxidation of 4-NP could only be obtained after 24 h of reaction (98% conversion). The analysis of the results obtained clearly emphasizes that the pillared clays have much superior catalytic activity than the natural clays towards the removal of 4-NP by CWPO. Therefore, the importance on the modification of natural clays by Zr, Fe and Cu cations to increase its catalytic activity in the CWPO of 4-NP is placed in evidence.
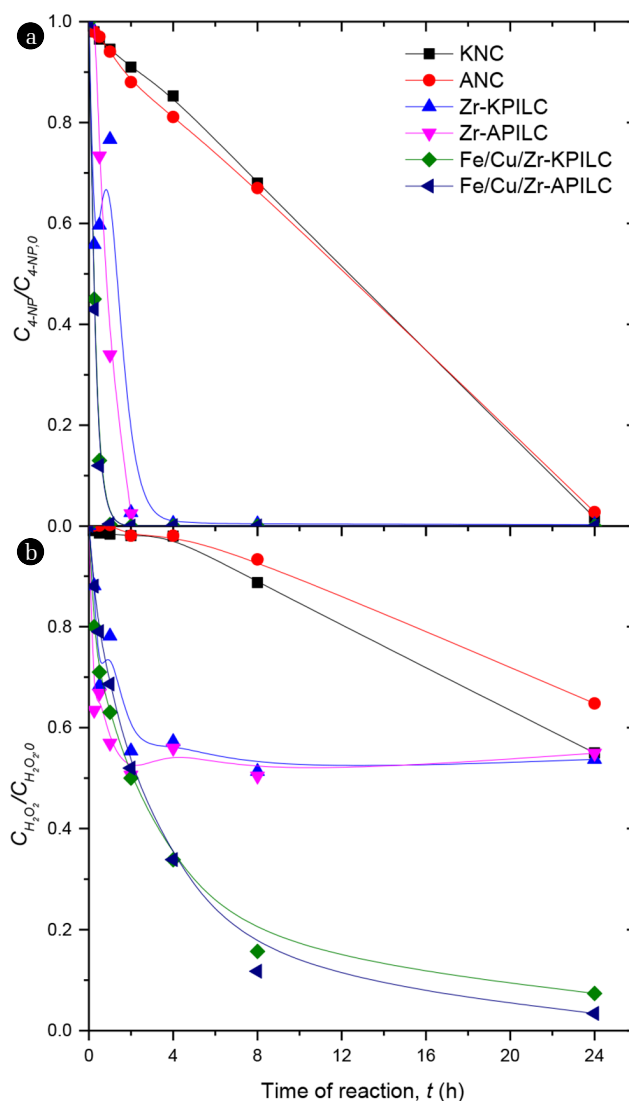

Fig. 4. Evolution of (a) 4-NP and (b) H$_2$O$_2$ against time of reaction by CWPO with the natural and pillared clays (Operating conditions: C_{4-NP} = 5 g L^{-1}, $C_{H_2O_2}$ = 17.8 g L^{-1}, C_{cat} = 2.5 g L^{-1}, initial pH = 3.0 and T = 50°C).

Fig. 4(b) shows the results obtained for H$_2$O$_2$ decomposition. It is clearly seen that the inclusion of Fe and Cu metals in the pillared clays drastically increases the activity of the materials for 4-NP oxidation. Nevertheless, the rate of H$_2$O$_2$ decomposition appears fairly similar for both Zr-KPILC and Zr-APILC during the first 4 h of reaction.

The conversion of 4-NP reached with any of the prepared PILCs is higher when compared with other catalysts used in previous works at the same operating conditions, such as graphene oxide materials [16] and carbon nanotubes [2]. The CWPO of 4-NP using clays as catalyst has been scarcely explored. Ayodele et al. [12] achieved a 4-NP degradation of 100% after 10 min, but using higher concentration of the catalyst and hydrogen peroxide (4 g L^{-1} of Cu-pillared synthetic bentonite with H$_2$O$_2$ in an excess of 20%

and light irradiation to assist the process) for much lower initial concentrations of 4-NP (75-100 ppm). Chirchi et al. [11] studied the degradation of similar initial concentrations of 4-NP (1 mM) in the presence of Fe- and Fe-Al-pillared synthetic bentonite (1 g L^{-1}), reaching complete conversions after 5 h. The prepared KPILC and APILC allow to completely remove high loads of 4-NP (5 g L^{-1}) in less time (2 h). The mineralization level obtained in the experiments was followed by measurements of the TOC conversion. The results obtained are represented in Fig. 5.

As expected, the removal of TOC is higher when pillared clays (conversion of TOC close to 70%) are used and compared to the natural clays. The highest TOC removal (65.1% after 8 h) was obtained with Fe/Cu/Zr-APILC. Under the same conditions, the
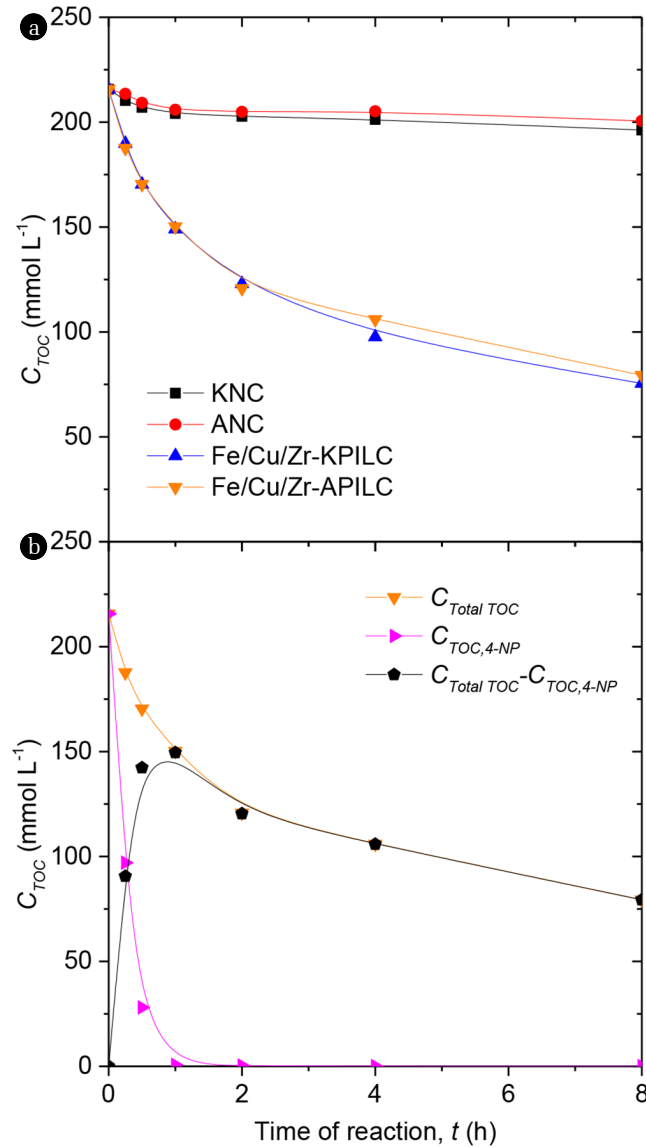

Fig. 5. Evolution of TOC removal in the CWPO of 4-NP with the (a) natural and Fe/Cu/Zr-PILCs and (b) Fe/Cu/Zr-APILC (Operating conditions: C_{4-NP} = 5 g L^{-1}, $C_{H_2O_2}$ = 17.8 g L^{-1}, C_{cat} = 2.5 g L^{-1}, initial pH = 3.0 and T = 50℃).
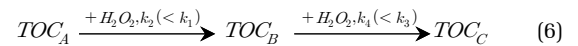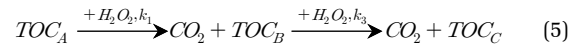
natural clays presented only 7.0% of TOC conversion after 8 h. After 24 h (results not shown), the removals of TOC were 74.5 and 78.5% with Fe/Cu/Zr-KPILC and Fe/Cu/Zr-APILC, respectively.

TOC conversions are considerably lower than 4-NP conversions, owing to the formation of more refractory products (intermediate compounds). Fig. 5(b) shows the evolution of TOC removal in the experiment carried out with Fe/Cu/Zr-APILC, detailing the experimental TOC of the reaction media ($C_{Total\ TOC}$), theoretical TOC of 4-NP (determined from the concentration of 4-NP by HPLC and taking into account its TOC contribution, $C_{TOC,4-NP}$) and, finally, the resultant TOC obtained by the subtraction of the $C_{TOC,4-NP}$ to $C_{Total,\ TOC}$, which can be considered as the TOC of the oxidizable intermediates and final refractory products. As can be observed, after 4-NP oxidation, oxidizable compounds are produced, since the $C_{Total\ TOC}$-$C_{TOC,4-NP}$ curve show a maximum concentration close to 1 h of reaction time. Then, when all 4-NP is almost removed, the $C_{Total\ TOC}$-$C_{TOC,4-NP}$ still decreases, evidencing the occurrence of oxidizable intermediates. According to previous works [16], the first stage leads to aromatic intermediates (4-nitrocathecol, phenol, hydroquinone, resorcinol, catechol and benzoquinone). Then these intermediates are further oxidized to low molecular weight carboxylic acids (malic, maleic, malonic, oxalic, acetic and formic acids), conferring to the aqueous media solution more acidity (final pH was found to be less than the initial pH of 3).

3.2.2. Kinetic modeling

Based on the TOC contributions described above (4-NP, oxidizable intermediates and refractory products), it is possible to describe the evolution of TOC by lumping into three blocks (TOC_A, TOC_B and TOC_C) to adjust the results to a simplified kinetic model (Eq. (4)-(6)).

$$C_{TOC} = C_{TOC,A} + C_{TOC,B} + C_{TOC,C} \tag{4}$$

$$TOC_A \xrightarrow{+H_2O_2,k_1} CO_2 + TOC_B \xrightarrow{+H_2O_2,k_3} CO_2 + TOC_C \tag{5}$$

$$TOC_A \xrightarrow{+H_2O_2,k_2(<k_1)} TOC_B \xrightarrow{+H_2O_2,k_4(<k_3)} TOC_C \tag{6}$$

TOC_A represents the initial TOC and, thus, TOC_A was assumed as the theoretical TOC of the 4-NP, $C_{TOC,4-NP}$, which is converted to CO_2 (justifying the decrease of TOC since the beginning of the CWPO process) and TOC_B, corresponding to the lump of the oxidizable intermediates. Once formed, these compounds also evolve to CO_2 and to the final refractory products, TOC_C. According with this, the following equations can be considered (Eq. (7)-(8)):

$$TOC_A = C_{Toc,4-NP} \tag{7}$$

$$TOC_B + TOC_C = C_{Total\ TOC} - C_{TOC,4-NP} \tag{8}$$

Simple power-law rate equations, of first reaction order with respect to each reactant (H_2O_2, TOC_A, TOC_B and TOC_C) have been checked for the prediction of H_2O_2 consumption and TOC removal,

Table 2. Kinetic Parameters Obtained in Modeling of CWPO of 4-NP with Natural and Pillared Clays

Catalyst	Kinetic parameters				
	$k_{H_2O_2}$ (L g^{-1} h^{-1})	k_1 (L g^{-1} h^{-1})	k_2 (L g^{-1} h^{-1})	k_3 (L g^{-1} h^{-1})	k_4 (L g^{-1} h^{-1})
KNC	0.062	0.037	0.024	0.128	0.128
ANC	0.038	0.041	0.031	0.080	0.080
Fe/Cu/Zr-KPILC	2.216	2.803	2.365	0.568	0.215
Fe/Cu/Zr-APILC	2.501	2.752	2.750	1.328	0.484

as follows (Eq. (9)-(12)):

$$-\frac{dC_{H_2O_2}}{dt} = k_{H_2O_2} \; C_{cat} \; C_{H_2O_2} \; C_{Toc} \qquad (9)$$

$$-\frac{dC_{TOC,4-NP}}{dt} = k_1 \; C_{cat} \; C_{H_2O_2} \; C_{TOC,4-NP} \qquad (10)$$

$$\frac{dC_{TOC,B}}{dt} = k_2 \; C_{cat} \; C_{H_2O_2} \; C_{TOC,4-NP} - k_3 \; C_{cat} \; C_{H_2O_2} \; C_{TOC,B} \quad (11)$$

$$\frac{dC_{TOC,C}}{dt} = k_4 \; C_{cat} \; C_{H_2O_2} \; C_{TOC,B} \qquad (12)$$

The numerical solution of these equations was solved by using the following initial conditions: $C_{H_2O_2} = C_{H_2O_2,0}$, $C_{TOC,4NP} = C_{TOC,4-NP,0}$, and $C_{TOC,B} = C_{TOC,C} = 0$ mol L^{-1} at $t_0 = 0$, in addition to consider that $C_{TOC} = C_{TOC,A} + C_{TOC,B} + C_{TOC,C}$. Table 2 summarize the values of the kinetic constants ($k_{H_2O_2}$ k_1, k_2, k_3 and k_4) proposed for the evolution of H$_2$O$_2$ and the lumped TOC in the CWPO of 4-NP with the natural and trimetallic-PILCs, according to Eq. (6)-(9). The values were determinate taking into account the concentration of the catalyst (2.5 g L^{-1}) based on the Eq. (1). The solution of the equations were achieved by minimizing the SSR, which summarized also in Table 2 in addition to the determination coefficient (R^2) for the simulated values of H$_2$O$_2$, 4-NP (as TOC of 4-NP) and TOC concentrations of reaction media.

As observed previously, the pillaring process increases substantially the catalytic activity of the clays in the CWPO of 4-NP, hence all kinetic constants obtained are significantly higher with Fe/Cu/Zr-PILCs when compared to the natural clays. In fact, the kinetic constants of hydrogen peroxide consumption ($k_{H_2O_2}$) and the first kinetic constants of TOC$_A$ removal (k_1) show values up to fifty times larger with the Fe/Cu/Zr-PILCs ($k_{H_2O_2}$, $k_1 > 2.2$ L g^{-1} h^{-1}) than those with the natural clays ($k_{H_2O_2}$, $k_1 < 0.07$ L g^{-1} h^{-1}), placing in evidence the far higher activity of the prepared PILCs when compared to the parent natural clays. The formation and oxidation of oxidizable organic intermediates (TOC$_B$) is also considerable larger using the Fe/Cu/Zr-PILCs ($k_2 > 2.3$ L g^{-1} h^{-1} and $k_3 > 0.5$ L g^{-1} h^{-1}, respectively), instead of the natural clays ($k_2 < 0.4$ L g^{-1} h^{-1} and $k_3 < 0.2$ L g^{-1} h^{-1}, respectively). The kinetic constant value relating the production of the refractory products (TOC$_C$) is also higher when PILCs are used ($k_4 > 0.2$ L g^{-1} h^{-1}). As expected, the kinetic constants relating to the formation of the subsequent lumped parts of TOC (k_2 for TOC$_B$ and k_4 for

TOC$_C$) are lower than the kinetic constants regarding the oxidation of the previous TOC blocks (k_1 and k_3, for the disappearance of TOC$_A$ and TOC$_B$, respectively). This is consequence of mineralization (formation of CO$_2$) or, in other words, the disappearance of TOC during the experiments. According to these results, the initial mineralization is higher when using Fe/Cu/Zr-KPILC ($k_1 = 2.803$ L g^{-1} h^{-1} and $k_2 > 2.365$ L g^{-1} h^{-1}) than with Fe/Cu/Zr-APILC ($k_1 = 2.752$ L g^{-1} h^{-1} and $k_2 > 2.750$ L g^{-1} h^{-1}), since the difference between the oxidation of TOC$_A$ (k_1) and formation of oxidizable intermediates, TOC$_B$, (k_2) is higher. It is also possible to observe that the oxidation rate of these compounds (TOC$_B$) show a lower kinetic constant when compared to the rate of disappearance of TOC$_A$ ($k_1 > k_3$), putting in evidence that the oxidized intermediates are harder to oxidize compared to 4-NP.

The determination coefficients (R^2) show a good agreement between the experimental and the simulated data for H$_2$O$_2$ and 4-NP concentrations. For TOC, a good determination coefficient is observed in the fitting of the experimental data obtained from Fe/Cu/Zr-PILCs. However, the regression of TOC does not show a good accuracy for the modelling of the data obtained with the natural clays (KNC and ANC). The results were maintained in order to compare the kinetic constant values obtained using the Fe/Cu/Zr-PILCs with the corresponding natural clays. Nevertheless, the proposed kinetic model, which was fitted for all experimental data, is able to represent the data with accuracy (Fig. S2). The validation of this model is also illustrated by the parity plots shown in Fig. S3.

The evolution of TOC lumped by three defined blocks (TOC$_A$, TOC$_B$ and TOC$_C$) with the Fe/Cu/Zr-PILCs is depicted in Fig. 6. As can be observed, the sum of the three contributions of TOC allows representing suitably the evolution of TOC removal, which is in agreement with the experimental data (as symbols). According to the kinetic model, the occurrence of TOC$_C$ (refractory products) is perceptible since the beginning of reaction. Interestingly, the model predicts significant differences between the pillared clays for TOC$_B$ and TOC$_C$ profiles, since TOC$_C$ production is faster with the Fe/Cu/Zr-APILC compared to Fe/Cu/Zr-KPILC.

This is consequence of a faster oxidation of TOC$_B$ (higher value of k_3 with Fe/Cu/Zr-APILC). Accordingly, TOC$_B$ evolution with Fe/Cu/Zr-APILC describes the maximum concentration value (24 min) before than Fe/Cu/Zr-KPILC (36 min). This means that the Fe/Cu/Zr-APILC is more active in the CWPO of 4-NP (the degradation of the pollutant is faster). However the concentration of TOC$_B$ with this catalyst at 8 h is close to 0 mmol L^{-1} and all TOC of the aqueous medium is consequence of the refractory products
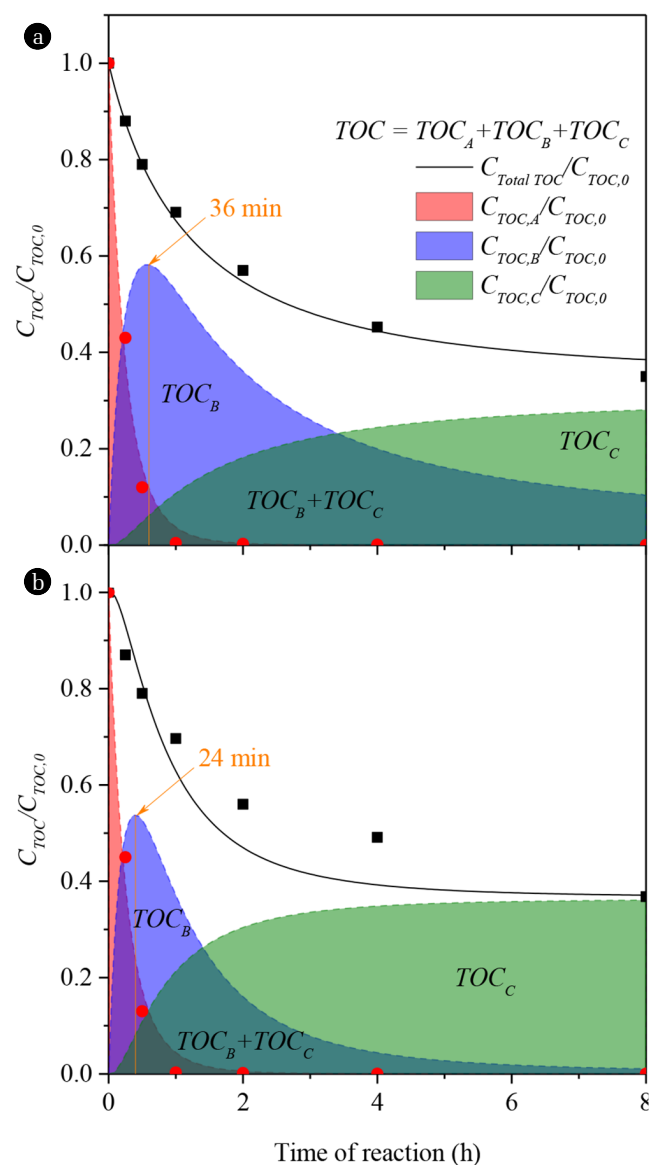
Fig. 6. Evolution of the simulated lumped TOC removal (symbols as experimental data of TOC and theoretical TOC contribution of 4-NP) in the CWPO of 4-NP with Fe/Cu/Zr-PILCs from (a) Karatau and (b) Akzhar (Operating conditions: $C_{4\text{-}NP}$ = 5 g L^{-1}, $C_{H_2O_2}$ = 17.8 g L^{-1}, C_{cat} = 2.5 g L^{1}, initial pH = 3.0 and T = 50°C).

(TOC_C), thus not more TOC can be degraded. On the other hand, the concentration of TOC_B is higher (10% of the initial TOC) at 8 h with Fe/Cu/Zr-KPILC, hence it is possible to achieve a higher mineralization, degrading this oxidizable TOC_B to be converted to TOC_C and CO_2.

4. Conclusions

Zr and Fe/Cu/Zr-PILCs were prepared from natural clays of Karatau

and Akzhar. The catalysts obtained by the simultaneous incorporation of Fe, Cu and Zr cations are highly efficient in the oxidation of 4-NP in aqueous medium at very mild conditions (50°C and atmospheric pressure). Pillared clay materials showed higher catalytic activity in the oxidation of 4-NP when compared to the natural clays. A complete removal of the contaminant is achieved after 4 h when Zr pillared clays are used, whereas the removal is reached after 2 h when Fe/Cu/Zr pillared clays are considered. The highest mineralization was obtained with the Fe/Cu/Zr-PILCs. By the subtraction of the theoretical organic carbon contribution of 4-NP to the measured TOC it is possible to observe the production of the oxidizable intermediates, since a maximum peak of concentration is observed. According to that, it is possible to propose a kinetic lumped model for TOC removal based in the initial TOC (corresponding to 4-NP), oxidizable intermediates and the refractory products. The kinetic model can be used to reproduce suitable the experimental data obtained in the CWPO of 4-NP with pillared clays.

Acknowledgments

References

1. Shibutov M. Industry report: Water management in Kazakhstan. In: Switzerland Global Enterprise. 2017.

2. Martin-Martínez M, Ribeiro RS, Machado BF, et al. Role of nitrogen doping on the performance of carbon nanotube catalysts: A catalytic wet peroxide oxidation application. *ChemCatChem* 2016;8:2068-2078.

3. Azabou S, Najjar W, Bouaziz M, Ghorbel A, Sayadi S. A compact process for the treatment of olive mill wastewater by combining wet hydrogen peroxide catalytic oxidation and biological techniques. *J. Hazard. Mater.* 2010;183:62-69.

4. Molina CB, Casas JA, Zazo JA, Rodriguez JJ. A comparison of Al-Fe and Zr-Fe pillared clays for catalytic wet peroxide oxidation. *Chem. Eng. J.* 2006;118:29-35.

5. Díaz de Tuesta JL, García-Figueruelo C, Quintanilla A, Casas JA, Rodriguez JJ. Application of high-temperature Fenton oxidation for the treatment of sulfonation plant wastewater. *J. Chem. Technol. Biotechnol.* 2015;90:1839-1846.

6. Catrinescu C, Arsene D, Teodosiu C. Catalytic wet hydrogen peroxide oxidation of para-chlorophenol over Al/Fe pillared

clays (AlFePILCs) prepared from different host clays. *Appl. Catal. B* 2011;101:451-460.

7. Mojović Z, Banković P, Milutinović-Nikolić A, Dostanić J, Jović-Jovičić N, Jovanović D. Al,Cu-pillared clays as catalysts in environmental protection. *Chem. Eng. J.* 2009;154:149-155.

8. Galeano LA, Vicente MA, Gil A. Catalytic degradation of organic pollutants in aqueous streams by mixed Al/M-pillared clays (M = Fe, Cu, Mn). *Catal. Rev.* 2014;56:239-287.

9. Cool P, Vansant EF. Pillared clays: Preparation, characterization and applications. Synthesis Springer. Berlin: Springer; 2001. p. 265-288.

10. Gil A, Korili SA, Trujillano R, Vicente MA eds. Pillared clays and related catalysts. 1st ed. New York: Springer-Verlag; 2010.

11. Chirchi L, Ghorbel A. Use of various Fe-modified montmorillonite samples for 4-nitrophenol degradation by H_2O_2. *Appl. Clay Sci.* 2002;21:271-276.

12. Ayodele OB, Hameed BH. Synthesis of copper pillared bentonite ferrioxalate catalyst for degradation of 4-nitrophenol in visible light assisted Fenton process. *J. Ind. Eng. Chem.* 2013;19:966-974.

13. Minz S, Garg S, Gupta R. Catalytic wet peroxide oxidation of 4-nitrophenol over Al-Fe, Al-Cu and Al-Cu-Fe pillared clays. *Indian Chem. Eng.* 2017;60:16-36.

14. Minz S, Garg S, Gupta R. Catalytic wet peroxide oxidation of 4-nitrophenol over Al-Fe PILC: Kinetic study using Fermi's equation and mechanistic pathways based on TOC reduction. *Chem. Eng. Commun.* 2018;205:667-679.

15. Zhang W, Xiao X, An T, et al. Kinetics, degradation pathway and reaction mechanism of advanced oxidation of 4-nitrophenol in water by a UV/H_2O_2 process. *J. Chem. Technol. Biotechnol.* 2003;78:788-794.

16. Ribeiro RS, Silva AMT, Pastrana-Martínez LM, Figueiredo JL, Faria JL, Gomes HT. Graphene-based materials for the catalytic wet peroxide oxidation of highly concentrated 4-nitrophenol solutions. *Catal. Today* 2015;249:204-212.

17. Ribeiro RS, Silva AMT, Figueiredo JL, Faria JL, Gomes HT. The role of cobalt in bimetallic iron-cobalt magnetic carbon xerogels developed for catalytic wet peroxide oxidation. *Catal. Today* 2017;296:66-75.

18. Diaz de Tuesta JL, Quintanilla A, Casas JA, Rodriguez JJ. Kinetic modeling of wet peroxide oxidation with a carbon black catalyst. *Appl. Catal. B* 2017;209:701-710.

19. Agency for toxic substances and diseases registry. Toxicologal profiles for nitrophenols: 2-nitrophenol, 4-nitrophenol. In: P.H.S. U.S. Dept. of Health & Human Services, Agency for Toxic Substances and Diseases Registry; 1992. p. 1-104.

20. U.S. Environmental Protection Agency. Nitrophenols–Ambient water quality criteria. 1980. p. A1-C134.

21. Newcombe G, Hayes R, Drikas M. Granular activated carbon: Importance of surface properties in the adsorption of naturally occurring organics. *Colloids Surf. A* 1993;78:65-71.

22. Diaz de Tuesta JL, Quintanilla A, Casas JA, Rodriguez JJ. P-, B- and N-doped carbon black for the catalytic wet peroxide oxidation of phenol: Activity, stability and kinetic studies. *Catal. Commun.* 2017;102:131-135.

23. Pinho MT, Silva AMT, Fathy NA, Attia AA, Gomes HT, Faria JL. Activated carbon xerogel-chitosan composite materials for catalytic wet peroxide oxidation under intensified process

24. Gomes HT, Figueiredo JL, Faria JL. Catalytic wet air oxidation of olive mill wastewater. *Catal. Today* 2007;124:254-259.

25. Ribeiro RS, Rodrigues RO, Silva AMT, et al. Hybrid magnetic graphitic nanocomposites towards catalytic wet peroxide oxidation of the liquid effluent from a mechanical biological treatment plant for municipal solid waste. *Appl. Catal. B* 2017;219:645-657.

26. Fatimah I. Preparation of ZrO_2/Al_2O_3-montmorillonite composite as catalyst for phenol hydroxylation. *J. Adv. Res.* 2014;5:663-670.

27. Bruckman VJ, Wriessnig K. Improved soil carbonate determination by FT-IR and X-ray analysis. *Environ. Chem. Lett.* 2013;11:65-70.

28. Djeffal L, Abderrahmane S, Benzina M, Fourmentin M, Siffert S, Fourmentin S. Efficient degradation of phenol using natural clay as heterogeneous Fenton-like catalyst. *Environ. Sci. Pollut. Res. Int.* 2014;21:3331-3338.

29. Munoz HJ, Blanco C, Gil A, Vicente MA, Galeano LA. Preparation of Al/Fe-pillared clays: Effect of the starting mineral. *Materials* 2017;10:1-18.

30. Carriazo JG, Guelou E, Barrault J, Tatibouët JM, Moreno S. Catalytic wet peroxide oxidation of phenol over Al-Cu or Al-Fe modified clays. *Appl. Clay Sci.* 2003;22:303-308.

31. Galeano LA, Gil A, Vicente MA. Effect of the atomic active metal ratio in Al/Fe-, Al/Cu- and Al/(Fe-Cu)-intercalating solutions on the physicochemical properties and catalytic activity of pillared clays in the CWPO of methyl orange. *Appl. Catal. B* 2010;100:271-281.

32. Khankhasaeva ST, Dashinamzhilova ET, Dambueva DV, Timofeeva MN. Catalytic properties of Fe-Cu-Al-montmorillonites in the oxidation of acid chrome dark blue azo dye. *Kinet. Catal.* 2013;54:307-313.

33. Zhou S, Zhang C, Hu X, et al. Catalytic wet peroxide oxidation of 4-chlorophenol over Al-Fe-, Al-Cu-, and Al-Fe-Cu-pillared clays: Sensitivity, kinetics and mechanism. *Appl. Clay Sci.* 2014;95:275-283.

34. Jia F, Su J, Song S. Can natural muscovite be expanded? *Colloids Surf. A* 2015;471:19-25.

35. Bohor BF, Randall EH. Scanning electron microscopy of clays and clay minerals. *Clays Clay Miner.* 1971;19:49-54.

36. Wan D, Wang G-H, Li W-B, Chen K, Shu G. Synthesis of Fe-Al pillared bentonite and heterogeneous Fenton degradation of orange. *Acta Physico-Chimica Sinica* 2013;29:2429-2436.

37. Li W, Wan D, Wang G, Chen K, Hu Q, Lu L. Heterogeneous Fenton degradation of Orange II by immobilization of Fe_3O_4 nanoparticles onto Al-Fe pillared bentonite. *Korean J. Chem. Eng.* 2016;33:1557-1564.

38. Tomul F. Influence of synthesis conditions on the physicochemical properties and catalytic activity of Fe/Cr-pillared bentonites. *J. Nanomater.* 2012;2012:1-14.

39. Tomul F, Turgut Basoglu F, Canbay H. Determination of adsorptive and catalytic properties of copper, silver and iron contain titanium-pillared bentonite for the removal bisphenol A from aqueous solution. *Appl. Surf. Sci.* 2016;360:579-593.

40. Tomul F. The effect of ultrasonic treatment on iron-chromium pillared bentonite synthesis and catalytic wet peroxide oxidation of phenol. *Appl. Clay Sci.* 2016;120:121-134.

41. Xue B, Guo H, Liu L, Chen M. Preparation, characterization and catalytic properties of yttrium-zirconium-pillared montmorillonite and their application in supported Ce catalysts. *Clay Miner.* 2018;50:211-219.

42. Mnasri-Ghnimi S, Frini-Srasra N. Effect of temperature synthesis on the catalytic performance of zirconium pillared interlayered clays for phenol oxidation. *Modern Chem. Applic.* 2017;5:1-9.